

Electric field-induced redistribution of free carriers at isotype (In,Ga)P/GaAs interfaces

P. Krispin^{a,*}, A. Knauer^b, S. Gramlich^b

^a Paul-Drude-Institut für Festkörperelektronik, Hausvogteiplatz 5-7, 10117 Berlin, Germany

^b Ferdinand-Braun-Institut für Höchstfrequenztechnik, Albert-Einstein-Str. 11, 12489 Berlin, Germany

Abstract

Metal–semiconductor contacts are applied to study depth-resolved electrical characteristics of Si- and Zn-doped GaAs/(In,Ga)P/GaAs heterojunctions by capacitance–voltage measurements. The measured depth profiles of the carrier concentration are compared with calculations based on solutions of the Poisson equation. Different growth conditions are chosen in order to produce heterointerfaces with (In,Ga)P layers of various degrees of order. It is shown that (In,Ga)P ordering induces piezoelectric polarization charges at interfaces with GaAs, the density of which increases with higher degree of order. The related electric field results in a redistribution of free carriers. For weakly ordered (In,Ga)P, the interfaces are found to be of type I. © 2002 Elsevier Science B.V. All rights reserved.

Keywords: (In,Ga)P ordering; Sheet charges; InGaP/GaAs interfaces

1. Introduction

The electronic properties of (In,Ga)P/GaAs interfaces are of crucial importance for potential applications in heterojunction bipolar transistors, high-electron-mobility transistors, light-emitting and laser diodes, and solar cells. Despite a large number of investigations, the characteristics of (In,Ga)P/GaAs heterointerfaces are still controversially discussed. Although it is known that (In,Ga)P exhibits a tendency to order, there are only a few studies on electrical properties of interfaces between GaAs and ordered (In,Ga)P [1–3]. The conduction band offset ΔE_C seems to decrease with increasing ordering [1]. Calculations however show that ordered (In,Ga)P has a strong piezoelectric polarization, which may largely modify the electronic characteristics of (In,Ga)P/GaAs interfaces [4]. Sheet charges and related electric fields are therefore expected, but not noted yet in experimental work on

interfaces between GaAs and ordered (In,Ga)P. For example, electron traps [2] and internal strain at interfaces [3] are discussed as sources of the strong electron depletion at n-type GaAs-on-(In,Ga)P interfaces.

Our investigations focus on Si- as well as Zn-doped normal [(In,Ga)P-on-GaAs] and inverted [GaAs-on-(In,Ga)P] heterointerfaces grown by metalorganic-vapor-phase epitaxy (MOVPE). Different growth conditions are chosen in order to produce heterointerfaces with (In,Ga)P layers of various degrees of order. The electrical properties of the lattice-matched heterojunctions are examined by the capacitance–voltage (C–V) method [5]. Based on solutions of the Poisson equation, one-dimensional simulations of the free carrier distribution at isotype heterojunctions are carried out [6], in order to determine concentration and sign of interfacial charges as well as conduction and valence band offsets ΔE_C and ΔE_V . It is experimentally shown that (In,Ga)P ordering induces piezoelectric polarization charges at interfaces with GaAs, the density of which rises with increasing degree of order. For weakly ordered (In,Ga)P, the interfaces are found to be of type I.

* Corresponding author. Tel.: +49-30-2037-7399; fax: +49-30-2037-7515.

E-mail address: krispin@pdi-berlin.de (P. Krispin).

2. Experimental details

The investigated GaAs/(In,Ga)P/GaAs heterojunctions were produced in a horizontal MOVPE reactor on highly doped GaAs substrates. In order to realize (In,Ga)P alloys with different degrees of order, the structures were grown at 580 °C on (001)-oriented GaAs [set A], at 650 °C on singular (001) substrates [set B], and at 650 °C on (001) substrates with a miscut of 2° towards (111)B [set C]. The growth conditions for sets A and C lead to weakly and strongly ordered (In,Ga)P layers, respectively. Samples of sets B and C, which were grown simultaneously, exhibit double- and single-variant ordered (In,Ga)P alloys, respectively [7]. Growth rates of 2.5 μm h⁻¹ and V/III input ratios of 70 were used. The interface regions were realized with growth interruptions of about 5 s. The lattice mismatch of the (In,Ga)P layers was in all cases below 5 × 10⁻⁴ at room temperature. Si- and Zn-doped layers were grown with carrier concentrations in the 10¹⁷ cm⁻³ range as determined by the C–V method. Secondary ion mass spectrometry (SIMS) was used to measure depth profiles of dopant density and composition. As metal–semiconductor (MS) contacts for the electrical measurements, Ti/Au dots were formed by electron beam deposition. An Ar⁺-laser was used as the excitation source for photoluminescence (PL) measurements.

The depth profiles of the electron (hole) concentration n (p) were measured at 1 MHz and 300 K using the conventional C–V method [5]. The concentrations n or p were obtained from the expression

$$n(W) \text{ or } p(W) = \frac{2}{A^2 q \epsilon \epsilon_0} \left[\frac{d}{dV} \left(\frac{1}{C^2} \right) \right]^{-1} \quad (1)$$

where W denotes the thickness of the space-charge layer below the MS contact, A the contact area, q the elementary charge, and $\epsilon \epsilon_0$ the dielectric constant. The depth W was calculated from the depletion capacitance C using $W(V) = \epsilon \epsilon_0 A / C(V)$. In order to scan the complete carrier concentration versus depth profile of isotype heterojunctions, the layer sequence was

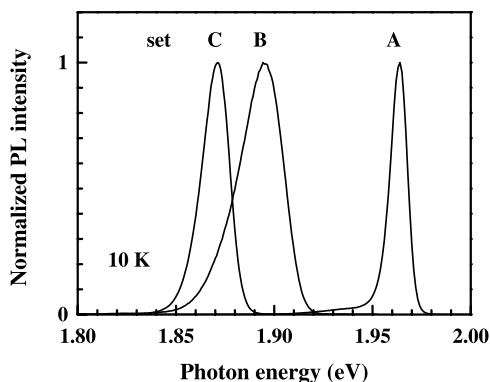


Fig. 1. Typical PL spectra of n-type (In,Ga)P layers at 10 K.

recess-etched a few times. By changing the d.c. bias in reverse direction, the edge of the space charge layer below the MS contact could thus be shifted across both interfaces of the GaAs/(In,Ga)P/GaAs heterostructures studied.

Based on solutions of the Poisson equation, one-dimensional simulations were carried out, in order to determine band offsets as well as amount and character of sheet charges at normal and inverted interfaces. The Poisson–Schrödinger solver of Snider et al. [6] was used to calculate capacitance versus voltage characteristics. Subsequently, calculated depth profiles of the carrier densities were obtained from Eq. (1).

3. Results and discussion

3.1. Photoluminescence

PL measurements at 10 K have been applied to measure the band gap reduction, which is associated with long-range ordering in (In,Ga)P [8,9]. Typical PL spectra of (In,Ga)P layers grown under conditions A, B, and C are displayed in Fig. 1. Changes of the peak energy are not linked with compositional variations, but are due to different degrees of order. The peak positions are equal for n- and p-type heterojunctions grown under similar conditions. It should be noted that we have found under certain growth conditions a maximal PL peak energy of 1.99 eV, which corresponds to the disordered (In,Ga)P alloy [9].

The PL bands in Fig. 1 are due to excitons, because the PL peak energies do not change, when the excitation intensity is increased [8,9]. Ignoring exciton binding energy and Stokes shift, which is commonly less than 15 meV for such bands [9], the PL peak energies in Fig. 1 can be used as a measure for the band gap of the differently ordered (In,Ga)P layers. The degree of order η defined as the average composition of alternating Ga- and In-rich planes along a 111 direction is calculated from the relation

$$E_G(0) - E_G(\eta) = 0.471\eta^2 \text{ (eV)} \quad (2)$$

which has been experimentally verified at low temperatures [8]. $E_G(\eta)$ denotes the band gap of (In,Ga)P with order parameter η . The degree of order varies from $\eta = 0$ for complete disordering to $\eta = 1$ for perfect ordering. For the (In,Ga)P layers of sets A, B, and C in Fig. 1, the η values are found to be 0.23, 0.45, and 0.50, respectively, with a maximum error of 0.03.

3.2. Depth profiles of carrier density

For (In,Ga)P-on-GaAs interfaces of n-type heterojunctions with different order parameters, typical depth profiles of the electron concentration n are depicted in

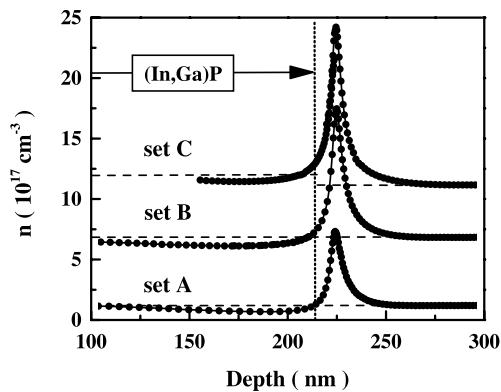


Fig. 2. Typical depth profiles of the electron concentration for normal n-type interfaces grown under conditions A, B, and C. The depth scales are normalized to an interface position of 215 nm (marked by dotted line). Horizontal dashed lines denote the constant doping levels in GaAs and (In,Ga)P. Curves are vertically shifted for clarity.

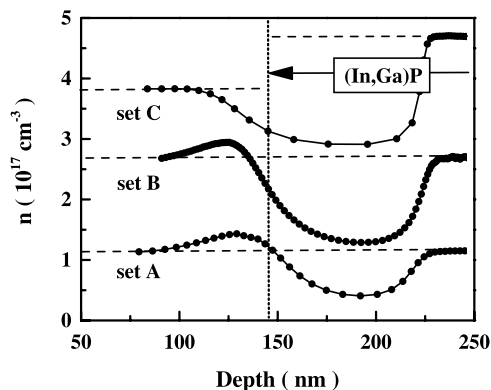


Fig. 3. Typical depth profiles of the electron concentration for inverted n-type interfaces grown under conditions A, B, and C. The depth scales are normalized to an interface position of 145 nm (marked by dotted line). Horizontal dashed lines denote the constant doping levels in GaAs and (In,Ga)P. Curves are vertically shifted for clarity.

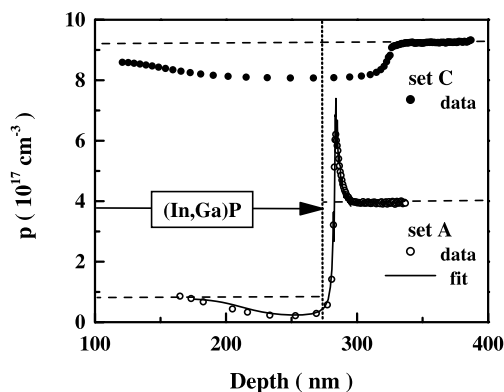


Fig. 4. Typical depth profiles of the hole concentration for normal p-type interfaces grown under conditions A and C. The line for sample A has been calculated (see text). The depth scales are normalized to an interface position of 275 nm (marked by dotted line). Horizontal dashed lines denote the constant doping levels in GaAs and (In,Ga)P. The curve for set C is vertically shifted for clarity.

Fig. 2. The common peak–valley structure of isotype heterojunctions is revealed. The conduction band edge of (In,Ga)P is above that of GaAs. The peak carrier concentration on the GaAs side grows with increasing order parameter η . When integrating the curves in Fig. 2, an excess of electrons over the doping level is found, which reaches $1.2 \times 10^{12} \text{ cm}^{-2}$ for (In,Ga)P-on-GaAs interfaces of set C. This surplus of electrons is related to a high density of positive sheet charges, which results in a drop of the conduction band at the normal interface. For higher ordered (In,Ga)P layers, the concentration of positive charges at the (In,Ga)P-on-GaAs interface apparently increases. These charges are not linked with deep levels, because we have never found interfacial states at n-type normal heterointerfaces by deep-level transient spectroscopy [10].

For GaAs-on-(In,Ga)P interfaces of n-type heterojunctions, characteristic depth profiles of the electron density are plotted in Fig. 3. In contrast to the normal interface, the peak concentration on the GaAs side is lower and decreases for interfaces with higher ordered (In,Ga)P. When the depletion on the (In,Ga)P side becomes dominant for set C samples, the electron accumulation on the GaAs side is missing. For n-type inverted interfaces, we always find a distinct electron depletion. For the samples of set A, B, and C in Fig. 3, we determine carrier deficits of 3.2×10^{11} , 8.6×10^{11} , and $13 \times 10^{11} \text{ cm}^{-2}$, respectively. The carrier depletion is due to negative sheet charges at these heterointerfaces, which lead to a rise of the conduction band edge. Interfacial electron traps are not observed and can be therefore neglected as a possible source for sheet charges [10].

For (In,Ga)P-on-GaAs interfaces of p-type heterojunctions, depth profiles of the hole density are plotted in Fig. 4. Whereas for the sample of set A the peak–valley structure of an isotype heterojunction is clearly seen, there is remarkable carrier depletion at the heterointerface with (In,Ga)P of set C. With increasing order, the hole deficit becomes larger than $1 \times 10^{12} \text{ cm}^{-2}$. The hole depletion originates from a high density of positive sheet charges, which lower the valence band at the normal interface. Comparing the (In,Ga)P-on-GaAs interface of the p-type sample (set A in Fig. 4) with the corresponding n-type junction in Fig. 2, it is obvious that the presence of positive charges at the normal interface does not depend on the conductivity type. At least for the p-type sample of set A in Fig. 4, it is seen that the valence band edge in (In,Ga)P is lower than that in GaAs. Together with the results on n-type heterojunctions grown under similar conditions (Fig. 2), we conclude that (In,Ga)P/GaAs interfaces of set A are of type I. Due to the strong hole depletion, similar conclusions cannot be drawn for interfaces with highly ordered (In,Ga)P.

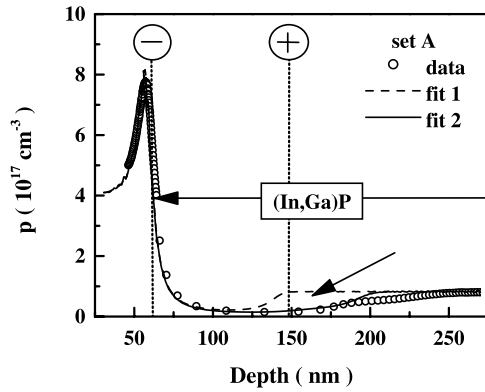


Fig. 5. Simulation of the hole distribution at the inverted p-type interface (set A). The experimental p versus depth profile (circles) is simulated by fits 1 and 2 (see text). The interface position and appearance of a positive sheet charge are marked by dotted lines at 62 and 147 nm, respectively.

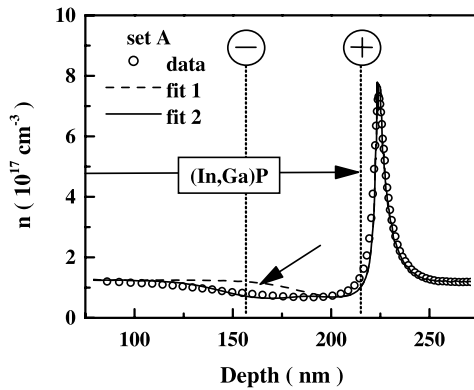


Fig. 6. Simulation of the electron distribution at the normal n-type interface (set A). The experimental n versus depth profile (circles) is simulated by fits 1 and 2 (see text). The interface position and appearance of a negative sheet charge are marked by dotted lines at 217 and 157 nm, respectively.

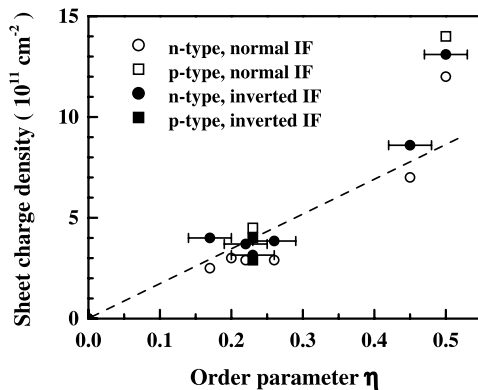


Fig. 7. Sheet charges at normal and inverted (In,Ga)P/GaAs interfaces versus order parameter η . Closed and open symbols denote negative and positive charges, respectively. For negative sheet charges, error bars of parameter η are depicted. The dashed line is a guide to the eye.

3.3. Simulation of carrier distributions

Information about band offsets and interface charges is gained by comparing the measured carrier distributions with calculated depth profiles. For the normal interface of a p-type heterojunction of set A, the simulation of the hole density is drawn as a line in Fig. 4. An excellent fit is obtained with a valence band offset ΔE_V of 0.28 eV and $4.5 \times 10^{11} \text{ cm}^{-2}$ positive sheet charges.

For the inverted interface of the same p-type heterojunction investigated in Fig. 4, the depth profile of the hole density is plotted in Fig. 5. The peak–valley structure of the isotype heterojunction is clearly revealed. Fit 1 (dashed line in Fig. 5) results from a calculation with a valence band offset ΔE_V of 0.32 eV and $3 \times 10^{11} \text{ cm}^{-2}$ negative sheet charges at the interface. This fit is perfect close to the interface. Additional holes are fixed at this interface due to negative sheet charges. Practically the same amount of negative charges is found at the inverted interface of n-type heterojunctions grown under conditions A (Fig. 3).

Inside the (In,Ga)P layer, there is a further hole depletion marked in Fig. 5 by an arrow. The decrease of the hole concentration towards the interface does not originate from spatial variations of the Zn concentration as checked by SIMS. The depletion around 150 nm is most likely linked with a positive sheet charge. When a positive charge density of $3.5 \times 10^{11} \text{ cm}^{-2}$ is incorporated at 147 nm, the experimental carrier distribution in Fig. 5 is fully matched by the calculated depth profile (fit 2).

The simulation for the normal interface of n-type heterojunctions (set A) is shown in Fig. 6 (cf. Fig. 2). Fit 1 (dashed line in Fig. 6) is calculated with a conduction band offset ΔE_C of 0.17 eV and $3 \times 10^{11} \text{ cm}^{-2}$ positive sheet charges at the interface. The calculation fits the measured carrier distribution only on the GaAs side. As for the p-type inverted interface (Fig. 5), carriers are missing inside the (In,Ga)P layer adjacent to the depletion region (marked by an arrow in Fig. 6). The electron deficit around 160 nm does not originate from variations of the Si doping level, but is likely due to a negative sheet charge. The depth profile of the electron concentration in Fig. 6 can be perfectly fitted, when a negative sheet charge of $2.5 \times 10^{11} \text{ cm}^{-2}$ is additionally incorporated at 157 nm (fit 2). This density approaches the concentration of positive charges, which is detected directly at the normal interface.

3.4. Order-induced interfacial charges

For the investigated interfaces, data are compiled in Fig. 7. The interfacial charge density increases with increasing order parameter η . We find for all sample sets positive and negative charges at normal and in-

verted interfaces, respectively. For similar growth conditions, the concentration of positive (negative) charges at normal (inverted) interfaces does not depend on the conductivity type. For the same sample, the absolute values of charge densities at normal and inverted interfaces are comparable, although the two interfaces are electrically screened. Deep-level defects with comparable densities are not found at the interfaces and can, thus, be excluded as sources of sheet charges. We therefore conclude that the charges found at (In,Ga)P/GaAs interfaces are associated with ordering in (In,Ga)P.

The experimental results can be completely explained by polarization charges in ordered (In,Ga)P. It is well known that ordered (In,Ga)P can exhibit strain-induced piezoelectric polarization [4,7]. The polarization difference between ordered (In,Ga)P and GaAs (no polarization) leads therefore to opposite sheet charges at normal and inverted (In,Ga)P/GaAs interfaces as observed. In a simplified model, the (In,Ga)P layers consist of several domains with ordered material in otherwise disordered (In,Ga)P [11]. Additional polarization charges are therefore expected inside the (In,Ga)P layer (cf., for example, Ref. [7]), which are usually screened by free carriers. Adjacent to the (In,Ga)P/GaAs interfaces, however, mirror charges of such domains inside (In,Ga)P can be observed (Figs. 5 and 6).

4. Conclusions

The order-induced sheet charges found in (In,Ga)P/GaAs heterojunctions have remarkable consequences for optical and electrical properties of structures with such interfaces. Because normal and inverted interfaces exhibit opposite charges, suitable design becomes important for devices. Whereas the interfacial charge density depends on the order parameter η , the charge character is determined by the growth sequence. Under the growth conditions applied, additional electrons (holes) can be generated in GaAs at normal (inverted) interfaces.

The large variation of data for (In,Ga)P/GaAs band offsets in the literature is mainly due to the fact that ordering and polarization charges have not been considered until now. For weakly ordered (In,Ga)P ($\eta \approx 0.23$), we independently determine ΔE_C and ΔE_V to be (0.20 ± 0.03) and (0.30 ± 0.03) eV, respectively, in agreement with the measured band gap difference ΔE_G of about 0.50 eV. The interfaces with weakly ordered (In,Ga)P are of type I, as expected from theoretical calculations [4]. For strongly ordered (In,Ga)P ($\eta \approx 0.50$), ΔE_C is also positive, in contrast to theoretical results for completely ordered material [4].

Acknowledgements

The authors would like to thank M. Gielow, H. Kantwerk, H. Kostial, and E. Wiebicke for technical assistance and H.T. Grahn for helpful comments and careful reading of the manuscript.

References

- [1] J.J. O'Shea, C.M. Reaves, S.P. DenBaars, M.A. Chin, V. Narayanamurti, *Appl. Phys. Lett.* 69 (1996) 3022.
- [2] T. Kikkawa, K. Imanishi, K. Fukuzawa, T. Nishioka, M. Yokoyama, H. Tanaka, *Inst. Phys. Conf. Ser.* 155 (1997) 877.
- [3] Y.H. Kwon, W.G. Jeong, Y.H. Cho, B.D. Choe, *Appl. Phys. Lett.* 76 (2000) 2379.
- [4] S. Froyen, A. Zunger, A. Mascarenhas, *Appl. Phys. Lett.* 68 (1996) 2852.
- [5] See, for example, P. Blood, J.W. Orton, *The Electrical Characterization of Semiconductors: Majority Carriers and Electron States*, Academic Press, New York, 1992.
- [6] I.H. Tan, G.L. Snider, L.D. Chang, E.L. Hu, *J. Appl. Phys.* 68 (1990) 4071.
- [7] J.K. Leong, C.C. Williams, J.M. Olson, S. Froyen, *Appl. Phys. Lett.* 69 (1996) 4081.
- [8] P. Ernst, C. Geng, F. Scholz, H. Schweizer, Y. Zhang, A. Mascarenhas, *Appl. Phys. Lett.* 67 (1995) 2347.
- [9] P. Ernst, C. Geng, F. Scholz, H. Schweizer, *Phys. Status Solidi (b)* 193 (1996) 213.
- [10] P. Krispin, M. Asghar, A. Knauer, H. Kostial, *J. Cryst. Growth* 220 (2000) 220.
- [11] A. Sasaki, K. Tsuchida, Y. Narukawa, Y. Kawakami, S. Fujita, Y. Hsu, G.B. Stringfellow, *J. Appl. Phys.* 89 (2001) 343.